AD743269

RELATION BETWEEN PARTICULATE CHEMISTRY

AND CERAMIC PROPERTIES

ANNUAL REPORT

1 January 1971 - 31 December 1971

Contract N00014-70-C-0138

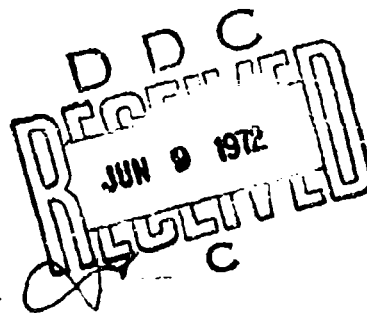AVSD-0155-72-CR

Prepared by

W.H. Rhodes
B.J. Wuensch
T. Vasilos

Prepared for

Office of Naval Research
Washington, D.C.   20360

Submitted by

AVCO CORPORATION
Systems Division
Lowell Industrial Park
Lowell, Massachusetts   01851

RELATION BETWEEN PARTICULATE CHEMISTRY

AND CERAMIC PROPERTIES

ANNUAL REPORT

1 January 1971 - 31 December 1971

Contract N00014-70-C-0138

AVSD-0155-72-CR

Prepared by

W.H. Rhodes
B.J. Wuensch
T. Vasilos

Prepared for

Office of Naval Research
Washington, D.C.   20360

Submitted by

AVCO CORPORATION
Systems Division
Lowell Industrial Park
Lowell, Massachusetts   01851

DOCUMENT CONTROL DATA - R&D

(Security classification of title, body of abstract and indexing annotation must be entered when the overall report is classified)

1. ORIGINATING ACTIVITY (Corporate author)	2a. REPORT SECURITY CLASSIFICATION
Avco Corporation	Unclassified
Space Div.sion	2b. GROUP
Lowell, Massachusetts 01851	

3. REPORT TITLE

Relation Between Particulate Chemistry and Ceramic Properties

4. DESCRIPTIVE NOTES (Type of report and inclusive dates)

Annual Report, 1 January 1971 - 31 December 1971

5. AUTHOR(S) (Last name, first name, initial)

Rhodes, William H.
Wuensch, Bernhardt J.
Vasilos, Thomas

6. REPORT DATE	7a. TOTAL NO. OF PAGES	7b. NO. OF REFS
December 31, 1971	26	29

8a. CONTRACT OR GRANT NO.	9a. ORIGINATOR'S REPORT NUMBER(S)
N00014-70-C-0138	
b. PROJECT NO.	
	9b. OTHER REPORT NO(S) (Any other numbers that may be assigned this report)

10. AVAILABILITY/LIMITATION NOTICES

Reproduction in whole or in part is permitted for any purpose of the U.S. Government. Distribution of this document is unlimited.

11. SUPPLEMENTARY NOTES	12. SPONSORING MILITARY ACTIVITY
	Dept. of the Navy
	Office of Naval Research
	Washington, D.C. 20360

13. ABSTRACT

Progress is described in the second year of a program designed to inter-relate the chemistry and morphology of the initial particulates with microstructure development and grain growth kinetics, impurity precipitate distribution and mechanical properties of the final product for both pure and doped MgO. Fine uniform grain size, high density >99.9% MgO samples were fabricated by vacuum hot pressing. Prior to this achievement an important inter-relationship between precursor and microstructure development was found. MgO crystallites derived from $Mg(OH)_2$ are crystallographically aligned with only small misorientations within an agglomerate which apparently is a relic of the parent brucite crystal. Crystallites within these agglomerates undergo very rapid grain growth during the intermediate stages of consolidation leading to exaggerated grain growth and highly abnormal structures. Powder derived from $MgCO_3$ is unoriented and allows normal grain growth to proceed during consolidation.

Equiaxed calcia-doped MgO samples were vacuum hot pressed from calcined co-precipitated $MgCO_3$ powder. Attempts to prepare $MgCO_3$ by freeze-drying were unsuccessful, but a very promising clacia-doped freeze-dried $Mg(C_3H_3O_2)_2$ was prepared. A dense calcia-doped specimen has been partially characterized leading to several intriguing features of the grain boundary second phase which need further characterization.

KEY WORDS	LINK A		LINK B		LINK C	
	ROLE	WT	ROLE	WT	ROLE	WT
Magnesium oxide						
Particulates						
Grain growth						
Impurity segregation						

INSTRUCTIONS

1. ORIGINATING ACTIVITY: Enter the name and address of the contractor, subcontractor, grantee, Department of Defense activity or other organization (corporate author) issuing the report.

2a. REPORT SECURITY CLASSIFICATION: Enter the overall security classification of the report. Indicate whether "Restricted Data" is included. Marking is to be in accordance with appropriate security regulations.

2b. GROUP: Automatic downgrading is specified in DoD Directive 5200.10 and Armed Forces Industrial Manual. Enter the group number. Also, when applicable, show that optional markings have been used for Group 3 and Group 4 as authorized.

3. REPORT TITLE: Enter the complete report title in all capital letters. Titles in all cases should be unclassified. If a meaningful title cannot be selected without classification, show title classification in all capitals in parenthesis immediately following the title.

4. DESCRIPTIVE NOTES: If appropriate, enter the type of report, e.g., interim, progress, summary, annual, or final. Give the inclusive dates when a specific reporting period is covered.

5. AUTHOR(S): Enter the name(s) of author(s) as shown on or in the report. Enter last name, first name, middle initial. If military, show rank and branch of service. The name of the principal author is an absolute minimum requirement.

6. REPORT DATE: Enter the date of the report as day, month, year; or month, year. If more than one date appears on the report, use date of publication.

7a. TOTAL NUMBER OF PAGES: The total page count should follow normal pagination procedures, i.e., enter the number of pages containing information.

7b. NUMBER OF REFERENCES: Enter the total number of references cited in the report.

8a. CONTRACT OR GRANT NUMBER: If appropriate, enter the applicable number of the contract or grant under which the report was written.

8b, 8c, & 8d. PROJECT NUMBER: Enter the appropriate military department identification, such as project number, subproject number, system numbers, task number, etc.

9a. ORIGINATOR'S REPORT NUMBER(S): Enter the official report number by which the document will be identified and controlled by the originating activity. This number must be unique to this report.

9b. OTHER REPORT NUMBER(S): If the report has been assigned any other report numbers (either by the originator or by the sponsor), also enter this number(s).

10. AVAILABILITY/LIMITATION NOTICES: Enter any limitations on further dissemination of the report, other than those

imposed by security classification, using standard statements such as:

(1) "Qualified requesters may obtain copies of this report from DDC."

(2) "Foreign announcement and dissemination of this report by DDC is not authorized."

(3) "U. S. Government agencies may obtain copies of this report directly from DDC. Other qualified DDC users shall request through

_____."

(4) "U. S. military agencies may obtain copies of this report directly from DDC. Other qualified users shall request through

_____."

(5) "All distribution of this report is controlled. Qualified DDC users shall request through

_____."

If the report has been furnished to the Office of Technical Services, Department of Commerce, for sale to the public, indicate this fact and enter the price, if known.

11. SUPPLEMENTARY NOTES: Use for additional explanatory notes.

12. SPONSORING MILITARY ACTIVITY: Enter the name of the departmental project office or laboratory sponsoring (paying for) the research and development. Include address.

13. ABSTRACT: Enter an abstract giving a brief and factual summary of the document indicative of the report, even though it may also appear elsewhere in the body of the technical report. If additional space is required, a continuation sheet shall be attached.

It is highly desirable that the abstract of classified reports be unclassified. Each paragraph of the abstract shall end with an indication of the military security classification of the information in the paragraph, represented as (TS), (S), (C), or (U).

There is no limitation on the length of the abstract. However, the suggested length is from 150 to 225 words.

14. KEY WORDS: Key words are technically meaningful terms or short phrases that characterize a report and may be used as index entries for cataloging the report. Key words must be selected so that no security classification is required. Identifiers, such as equipment model designation, trade name, military project code name, geographic location, may be used as key words but will be followed by an indication of technical context. The assignment of links, rules, and weights is optional.

TABLE OF CONTENTS

LIST OF ILLUSTRATIONS

LIST OF TABLES

ABSTRACT

Progress is described in the second year of a program designed to inter-relate the chemistry and morphology of the initial particulates with microstructure development and grain growth kinetics, impurity precipitate distribution and mechanical properties of the final product for both pure and doped MgO. Fine, uniform grain size, high density $\geq$ 99.99% MgO samples were fabricated by vacuum hot pressing. Prior to this achievement an important inter-relationship between precursor and microstructure development was found. MgO crystallites derived from $Mg(OH)_2$ are crystallographically aligned with only small misorientations within an agglomerate which apparently is a relic of the parent brucite crystal. Crystallites within these agglomerates undergo very rapid grain growth during the intermediate stages of consolidation leading to exaggerated grain growth and highly abnormal structures. Powder derived from $MgCO_3$ is unoriented and allows normal grain growth to proceed during consolidation.

Equiaxed calcia-doped MgO samples were vacuum hot pressed from calcined co-precipitated $MgCO_3$ powder. Attempts to prepare $MgCO_3$ by freeze-drying were unsuccessful, but a very promising calcia-doped freeze-dried $Mg(C_3H_3O_2)_2$ was prepared. A dense calcia-doped specimen has been partially characterized leading to several intriguing features of the grain boundary second phase which need further characterization.

I. INTRODUCTION

Many technologically important properties of ceramics are determined by their microstructure. Mechanical properties are but one notable example. The microstructure obtained in a body is, in turn, dependent upon a number of kinetic processes which occur during fabrication; grain growth and changes in pore size, distribution and morphology. Grain boundaries are involved in all of these processes. In spite of the importance of boundary behavior, much remains to be learned about the kinetics of boundary migration and the interaction of boundaries with pores and impurities. In particular, little is known about the chemical state of grain boundaries in ceramic systems and the way in which this chemical state is related to the chemistry of the initial particulates from which a body is formed. It has only been recently appreciated, for example, that impurity segregation at boundaries is common in ceramic systems even when the impurities are present in concentrations as low as 30 ppm.[1] Segregation may give rise to enhanced mass transport at grain boundaries[2] and, thus, completely modify the kinetics of processes such as creep, oxidation, electrical conduction and sintering. Segregation is similarly known to directly affect strength and mechanical behavior.[3] On a second level, impurity segregation influences microstructure development and thus, through its influence during processing, may control final properties which are dependent upon micro-structure. An example is the intentional addition of small amounts of impurity to retard grain growth during sintering. This prevents the entrapment of pores within grains and thereby has permitted sintering of oxides to full theoretical density which have optical properties heretofore unobtainable.

Few studies of ceramic materials have been directed toward a funda-mental understanding of the physical and chemical state of grain boundaries.

Characterization of grain boundaries, especially in terms of chemistry, has usually been slighted in the evaluation of boundary-sensitive properties. The relation between the chemical state of the initial particulates and the segregation and distribution of impurities in the resulting micro-structure has been incompletely studied.

II. OBJECTIVES OF THE PRESENT PROGRAM

The present report is the Second Annual Report in the second year of a program designed to inter-relate mechanical properties, microstructure evolution and impurity precipitate distribution, on the one hand, with the chemistry and characteristics of the initial particulates. Magnesium oxide has been selected for study for a number of reasons. The material is of considerable technological importance. Several studies of grain growth kinetics have been performed with this oxide which are in conflict and point out the need for clarification, with well-characterized material, of the roles of trace amounts of porosity and impurities. Further, diffusion data are available for many of the important impurity cations normally present in MgO (e.g., Ca, Fe and Al) and these results will be of value in the interpretation of rates of impurity segregation and redistribution.

The specific aims of the program are,

1. The preparation and characterization of ultra-pure MgO particulates and also particulates which have been homogeneously doped with controlled amounts of cation impurity,

2. Consolidation of the particulates into fully dense bodies having both fine and uniform grain size,

3. Measurement of isothermal grain growth kinetics for both ultra-pure and doped materials,

4. Determination of impurity precipitate concentration and distribution at various stages of microstructure evolution, and

5. Correlation of microstructure and impurity precipitate distribution with stress corrosion behavior.

Previous studies of grain growth in magnesia have differed greatly, and the disparities are undoubtedly due to impurity effects and minor levels of porosity. It is, thus, important that definitive data be available for ultra-pure, fully-dense magnesia, since these measurements will serve as the standard with which subsequent studies of doped material will be contrasted. Work during the first year of the program was accordingly concentrated on the preparation, characterization and consolidation of ultra-pure MgO. This work has continued, but work was also initiated toward the preparation of doped material as well.

III. THEORY AND PREVIOUS RESULTS

3.1 Powder-Microstructure Control

The properties required of the finished microstructure dictate the use of high purity ($> 99.99\%$) particulates of an average particle size < 0.5 μm. A world-wide search revealed that MgO powder of this quality was not available, but that high purity $Mg(OH)_2$ and $MgCO_3$ could be purchased. Gordon and Kingery[4] had shown that MgO nuclei formed coherently within the $Mg(OH)_2$ lattice and subsequent growth set-up large strains, causing extensive fracturing and a resultant fine MgO powder. This approach showed promise toward achieving the required fine particulate size. Studies of high purity $Mg(OH)_2$ (50 ppm impurities by emission and 350 ppm impurities by spark source mass decomposition in the electron beam confirmed the topotatic nature of the decomposition where the (110) and (111) of the new MgO crystallites were parallel to the prism and basal planes, respectively, of the hexagonal brucite parent crystal. The distribution of particle sizes produced in a typical $1200^{\circ}C$ - 1 hour dynamic calcine had a mean particle size of 360 A$^{\circ}$ and was found to follow a log-normal

distribution as expected for a normal nucleation-and-growth process.

A number of samples were vacuum hot pressed to approximately 99.5% density; however, all bodies produced from $Mg(OH)_2$ derived MgO displayed a duplex microstructure consisting of nests of fine grains amongst much larger grains. (At the very highest hot pressing temperature, $1450^\circ C$, contrary to customary experience, the structure reverted to a large-grained normal grain size distribution.) By interrupting the densification cycle, samples at various levels of density were obtained for study, and it was shown that the tendency for duplex grain growth began below a level of 70% relative density in the consolidation cycle.

Because of the difficulty in achieving a normal grain structure in $Mg(OH)_2$ derived MgO, work was initiated using moderate purity (400 ppm impurities by emission spectrography) MgO derived from $MgCO_3$. Also, calcining studies were conducted on reagent grade $MgCO_3$ to determine if there was a correlation between the decomposed particulate/agglomerate structure and the hot pressed microstructure. The dense microstructures were almost uniformly normal for these samples. Further, the grain sizes were smaller by up to a factor of 30 for these samples compared to those fabricated by $Mg(OH)_2$ derived powder.

In a discussion of these studies[5] it was reasoned that the main difference for the resulting microstructures from the two base powders was due to a high degree of mutual orientation in crystallites within an agglomerate for powders derived from $Mg(OH)_2$. $MgCO_3$ has a larger molai volume decrease and although the decomposition mechanism was not studied in detail, the cube-shaped MgO crystallites were diffuse and randomly oriented to one another. Thus, it was thought that the secondary grain growth in $Mg(OH)_2$ derived MgO was nucleated by rapid growth of oriented crystallites within an agglomerate which were relics of the precursor.

Oriented crystallites could display the rapid growth found for the growth of coherent boundaries in solid bodies. Conversely, the lack of abnormal grain growth in $MgCO_3$ derived MgO was mainly due to the random crystallite orientation. However, this hypothesis was subject to question because, 1) the large differences in purities for MgO derived from the two salts could influence grain growth during consolidation, 2) the $MgCO_3$ derived MgO had been stored for over a year leading to the speculation that absorbed species such as CO_3^{-2}, OH^{-1}, etc., could influence growth and 3) one 6 μm grain size 99.9% dense sample fabricated from $MgCO_3$ derived material had a microstructure bordering on abnormal.

Experiments were conducted during this period to answer the above questions, establish the cause of abnormal grain growth, and learn how to process high density, high purity, uniform fine grain size material for properties studies.

3.2 Grain Growth

Grain growth was selected as one boundary-sensitive property for measurement and correlation. Normal grain growth describes a process in which the average grain size of a strain-free material increases continuously with time at elevated temperature without appreciable change in the distribution of grain sizes. For normal grain growth in a pure, fully dense system, a theory due to Turnbull[6] predicts;

$$D^2 - D_o^2 = (K\gamma V)t$$

where D is the average grain diameter, D_o is the initial grain diameter, K is a rate constant, γ in the interfacial energy, V is molar volume and t is time.

In non-ideal systems either the migration rate of pores,[7,8] the diffusion of solid solution impurities[9] ("impurity drag"), or precipitation

of second phase may control grain-growth kinetics.[10] Brook[11] has
considered the microstructural conditions for which each effect might
be expected to be dominant. His results show that control by boundary
mobility is to be expected when pores are small. Separation of boundaries
from pores (pore entrapment), is to be expected when the pore velocity
becomes less than the boundary velocity and will occur at large grain
sizes and when the pores are large and widely dispersed. Porosity-
controlled grain growth occurs at small grain sizes and when the pores are
large and close together. The effect of impurity is to increase the
mobility of pore relative to that of the boundary and thus, for a given
grain size, inci e the boundary-controlled region of behavior at the
expense of the pore entrapment region.

Several studies of grain growth in magnesia have been conducted,
but the influence of porosity and impurity on the process is not clear.
Measurements by Daniels et al[12] were among the first to be conducted on
a ceramic oxide. The data indicated normal grain growth, but the measure-
ments were complicated by the presence of considerable porosity and attendant
densification during annealing of the specimens. Subsequent measurements
at Avco[13] were the first to be conducted with a fully dense oxide. The
kinetics of normal grain growth were again observed but, in the absence
of porosity, growth rates were 4 to 6 times more rapid. Addition of 1%
Fe or Ti impurity to magnesia[14] produced grain growth rates much smaller
than those observed in earlier studies of either the porous[12] or fully
dense compacts[13] and, further, a change to a time dependence of 1/4 and
1/3 for the Fe and Ti additions, respectively.

A detailed study of grain growth in pure and Fe_2O_3-doped magnesia
with objectives similar to, but not identical with, the present work was

recently reported by Gordon et al[15] during the course of this program. Their results may be summarized as follows. Pure MgO did not exhibit the $t^{\frac{1}{2}}$ dependence of earlier studies, but exhibited an exponent which decreased with time. Grain growth was probably controlled by porosity in pure magnesia at all temperatures even though the amounts of porosity were small (less than 1%). The addition of Fe_2O_3 decreased the rate of grain growth and tended to stabilize normal grain growth kinetics.

Preliminary grain growth studies were conducted on 34 μm grain size high density, high purity MgO derived from $Mg(OH)_2$. As noted above, this large grain size material displayed a normal grain size distribution. Measurements at two temperatures exhibited a marked decay in growth at long times. The decay was similar to that found by Gordon et al[15] and was thought to be due to a transition from boundary controlled to pore controlled and finally to the onset of abnormal grain growth. This suggested that to measure boundary-controlled grain growth in high purity MgO over a sufficiently long period to describe the kinetics will require a completely dense sample.

The other significant point from the preliminary study was that the initial growth rate was faster than that found for any of the previous studies in MgO. This is additional evidence for boundary control over grain growth as it would imply that high purity material exerts less grain boundary drag as predicted.

3.3 Stress Corrosion

The second boundary-sensitive property to be investigated is stress corrosion. MgO is one of the few systems investigated to date where it has been shown that grain boundary impurities play a role in stress corrosion.[16] Further, it is predicted that this mechanical property in preference to any other mechanical property can be quantitatively correlated with grain boundary impurities.

Stress corrosion cracking is a well-known phenomena that is controlled by mechanical or chemical processes occurring at the interface between the solid and the environment. Under some conditions, the surface reaction can be beneficial, i.e., the Joffe's effect where dissolution increased the crack tip radius thereby blunting a potential critical crack. In most cases the surface reaction degrades the usable strength and, consequently, knowledge of such reactions is important for structural materials. There are two major classes of models governing the advancement of the stress corrosion crack; 1) those which postulate crack advancement by stress enhanced chemical dissolution at the tip - the point of highest chemical potential and, 2) those which involve only mechanical phenomena such as mobile dislocations or reduction of the surface energy term in the Griffith relationship.

Charles[17] performed a cursory study of stress corrosion in single crystal MgO. He found evidence for stress corrosion at 240°C testing under compression in dry nitrogen and saturated water vapor. Similar tests at room temperature gave mixed behavior. Considering the known hydration behavior of MgO, they speculated that stress corrosion in the classic manner for glass had occurred.

In contrast, there is abundant information that dislocation motion plays a role in fracture at room temperature and above. Higher fracture stresses and decreased ductility have been observed when single crystal surfaces have been chemically polished[18,19] which is thought to be a result of removing mobile dislocations normally introduced through handling damage. Similar results have been observed in bicrystals and high density polycrystalline magnesia.[19] Tensile strengths of over 100,000 psi were observed for fresh dislocation-free single crystals and bicrystals while a tensile strength of 35,000 psi was reported for polycrystalline material[19]

with a similarly prepared surface. Rice[20] examined fracture surfaces on extruded MgO having a pronounced (100) texture, and concluded that fracture was initiated from some point to 2 to 8 grains deep in the specimen by the intersection of slip bands and subsequent nucleation of a crack. Westwood et al[21] introduced dislocation half-loops on freshly cleaved MgO and studied the effect of adsorbed species on dislocation mobilities. He was principally interested in explaining the delayed creep phenomena found by Westbrook and Jorgenson.[22] Complexes of high positive or negative charge or molecules of high dipole moment significantly enhanced dislocation mobility giving what is termed a Rebinder effect. Thus, dislocation velocity is apparently influenced by environment and a mechanism for a delayed dislocation nucleated brittle fracture in MgO may be forwarded.

The authors[16] performed stress corrosion studies in an H_2O environment on two hot pressed grades and one sintered grade of polycrystalline MgO. Classic stress corrosion curves were found that could be interpreted by the stress corrosion mechanism of Charles and Hillig.[23] An activation volume of 1.37 cc/mole and reactants surface energy of 68 ergs/cm^2 were calculated for one grade of hot pressed material. However, the three materials tested showed marked differences in slope and intercept on the stress corrosion curve. Also, electron microscope examination revealed thin grain boundary phases in all three materials, and in one case, the phase was shown to be $Na_6Al_4Si_4O_{17}$. These results led to the conclusion that H_2O stress corrosion behavior was extrinsic and probably related to grain boundary impurities. As a method of differentiating between a chemical and mechanical stress corrosion model, tests were also conducted in dimethyl formamide (DMF) and a 10% solution of DMF in dimethyl sulfoxide. These solutions had been shown by Westwood to exhibit maxima and minima

respectively, in MgO dislocation mobilities. These tests exhibited increasing stress corrosion resistance in the order H_2O, DMF and DMSO-10% suggesting in addition to the conclusions noted above, that in the absence of H_2O dislocations play a role in a mechanical stress corrosion mechanism. It was predicted that truly single phase MgO would not be as sensitive to stress corrosion by H_2O and may be controlled by a mechanical stress corrosion mechanism in all of the above environments.

IV. PROGRAM PROGRESS

4.1 Relationship Between Precursor and Microstructure

The inter-relationship between precursor compound and the hot pressed microstructure was pursued since it was one of the most important findings on the program to date as outlined in Section 3.1, and several unanswered questions remained to be answered. It was important to answer these questions to establish firmly the tentative conclusions for achieving high purity, high density fine grain size normal structures for property studies. The initial experiment was to establish whether or not the marked duplex structure noted for the $Mg(OH)_2$ derived material compared with the normal structure for $MgCO_3$ derived material could have been due to the lower purity of the starting $MgCO_3$ powder.

The identical ultra-high purity $Mg(OH)_2$ powder used for all the studies described previously[5] was converted to $MgCO_3$ taking precautions to protect chemical integrity. $Mg(OH)_2$ was dissolved in HNO_3 and precipitated with NH_4CO_3. The $MgCO_3$ was calcined at 1100°C for 1 hour, conditions that were developed during the previous effort[5] to produce a crystallite size of about 300 A°. This powder was then pressure sintered under conditions that produced duplex structures in the ultra-high purity $Mg(OH)_2$ derived MgO. The microstructures of the two MgO samples are shown in Figure 1.

#5412-4 (a) 750X

#5525-3 (b) 750X

Figure 1. Microstructures of MgO Prepared from (a) High Purity $Mg(OH)_2$ and (b) same $Mg(OH)_2$ Converted to $MgCO_3$ before Calcining.

Hot Pressing Conditions and Results

SH182 $Mg(OH)_2 \longrightarrow MgO$
1200°C - 1 hr. dynamic calcine. 1255°C - 15 Kpsi - 30 min. 3.60 gm/cc - 16 μm grain intercept.
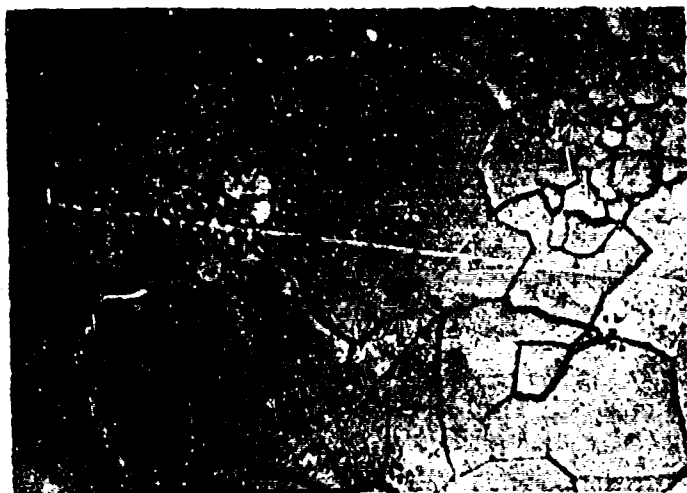
SH182 $Mg(OH)_2 \longrightarrow MgCO_3 \longrightarrow MgO$
1100°C - 1 hr. calcine. 1250°C - 15 Kpsi - 90 min. 3.566 gm/cc - 3.4 μm grain intercept.

The contrast in the microstructures is quite dramatic. The $MgCO_3$ derived material resulted in a much smaller grain size with a normal distribution. The average grain intercepts for the two samples are 16 μm and 3.4 μm indicating much more rapid growth for the $Mg(OH)_2$ derived sample. It was at peak temperature for 60 minutes less than the $MgCO_3$ derived sample further emphasizing the rapid growth for this sample. It is also of interest to compare the grain size of the fine grain patch in Figure 1a with the matrix of Figure 1b. This patch has an average grain intercept of 3.1 μm which was very close to the value exhibited for the entire matrix of the $MgCO_3$ derived material.

This experiment suggests that impurity content was not the dominant factor in the development of a normal microstructure for $MgCO_3$ derived material. It is very difficult to devise a completely unambiguous experiment, and this experiment suffers from the possibility that, in spite of efforts to protect chemical integrity, some contamination may have occurred during the solution-precipitation-calcination steps. Even the most sophisticated chemical analysis would not alleviate concern over this point. However, within these constraints, it now appears that the random orientation of crystallites as developed when calcining $MgCO_3$ is the prime requisite for developing a normal microstructure in a consolidated sample.

One experiment was conducted on the Honeywell M-10 moderate purity $MgCO_3$ derived MgO. This material had been stored in the calcined condition for over a year. Thus, it was hypothesized that absorbed atmospheric species such as OH^- or CO_3^{-2} could be playing a role in the microstructure development. Fifteen grams of the M-10 powder was dynamically calcined for 30 minutes at 1000°C in a partial vacuum. The powder charge was extracted

from the hot furnace, loaded into the die and quickly placed into the
vacuum hot pressing chamber. The entire procedure was designed to
volatilize adsorbed species and minimize resorption. The sample was
vacuum hot pressed under conditions that were found to be favorable for
achieving high density in the M-10 powder. The microstructure of this
sample is compared with a sample produced from the same powder without the
final desorption treatment in Figure 2.

The grain sizes are slightly different, but this undoubtedly relates
to the different times at maximum temperature. The main feature of
interest was the grain size distribution and number of equilibrium grains
(average of six sides). Both structures look abnormal. Microstructures
that look normal to the trained eye in practice usually possess a logarithmico-
normally distributed structure in three dimensions.[24] Quantitative grain
size distribution curves were not constructed for the two samples, but
counts of grain edges revealed 25% and 20% of the grains had > 6 sides for
the samples shown in Figure 2a and 2b, respectively, which, of course, is
indicative of an abnormal grain structure. The higher percentage of
> 6 sided grains in Figure 2a would indicate that this tendency increases
with annealing time. This argues for secondary grain growth being the
cause of the abnormal growth as opposed to a mechanism involving incomplete
primary recrystallization or oriented crystallites within agglomerates.

This experiment argues against adsorbed species exerting a strong
influence over microstructure development. Such effects as has been
suggested by Rice,[25] may influence properties, but in this case they do
not appear to exert subtle effects on microstructure development. The
secondary grain growth found for these two $MgCO_3$ derived samples is
altogether different than the widely varying duplex structure found in the
$Mg(OH)_2$ derived material. This secondary growth is probably caused by
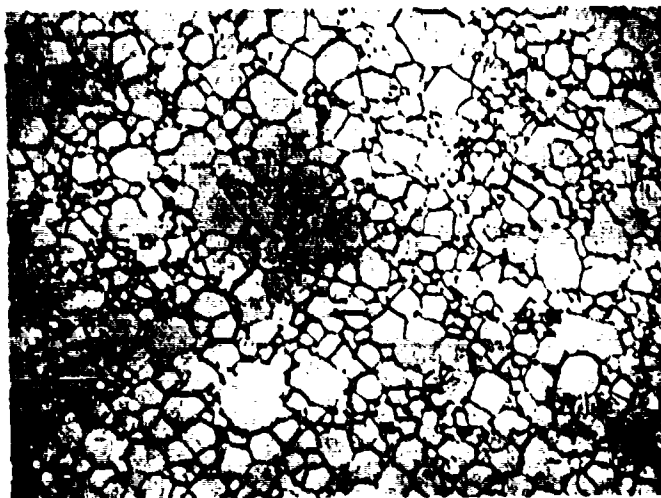
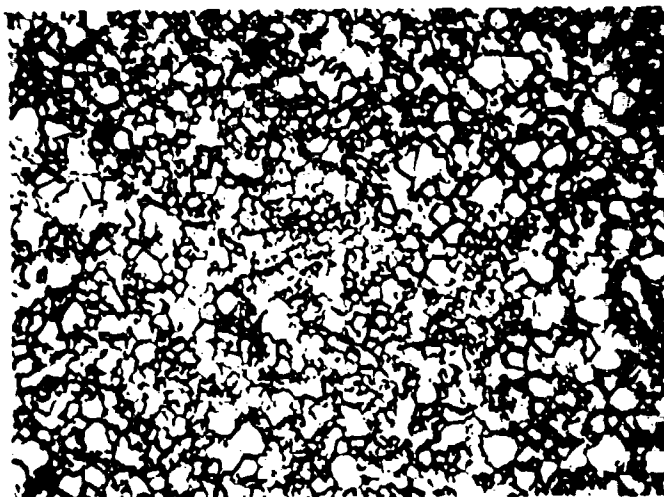#5412-5   (a)   500X

Honeywell - M10
As-recieved
Hot Pressed

1250°C - 15 Kpsi -
90 min. 3.585 gm/cc -
6 μm grain intercept

#5435   (b)   500X

Honeywell - M10
Dynamically Calcined
1000°C - 30 min.
Hot Pressed

1250°C - 15 Kpsi -
60 min. - 3.591 gm/cc -
4.2 μm grain intercept

Figure 2. Microstructure of MgO Prepared from
           MgCO$_3$ Derived Powders Treated in
           Different Ways.

the usual mechanism in ceramics. That is, the nucleation of secondary grains is caused by more rapid boundary mobility due to a lack of restraint such as impurities or pores. Once a >6 sides grain nucleates, it continues to grow rapidly due to the increased driving force caused by the increased curvature.
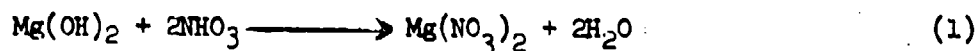
4.2 Preparation of Doped Magnesia

A major effort was devoted to the development of satisfactory chemical processes for preparing doped powders. Specific concentrations of the dopant were required as well as a uniform atomic dispersion of dopant. The traditional ceramic processes of blending and calcining were rejected because of the desire for an atomic dispersion of solute and the requirement for a fine particulate size that could be consolidated to a fine uniform grain high density structure. Thus, the specifications for the powder were similar to that required for the high purity powder previously discussed with the additional doping criteria.

Freeze-drying was selected as the principal process for investigation. Some work was also accomplished on co-precipitation which was a direct outgrowth of the basic freeze-drying experiments. A freeze-drying apparatus was constructed in this laboratory that was consistent with practice described in the literature.[26,27] An argon gas forces the salt solution through the aerosol nozzle into a stirred -76°C hexane solution contained in a vacuum flask cooled by dry ice and acetone. After decanting the hexane, the same vacuum flask is connected to a vacuum system having a large liquid N_2 trap (-196°C) for collecting water and hexane. After several hours the powder is ready for the next step in the process, calcining.

Initially, the chemistry of various magnesia salt solutions was explored. The first experiments were based on trying to end up with a

carbonate as has been previously discussed, hot pressing had demonstrated that this salt was desirable as an MgO precursor. The chemistry of forming a carbonate is as follows:

$$Mg(OH)_2 + 2NHO_3 \longrightarrow Mg(NO_3)_2 + 2H_2O \qquad (1)$$

$$Mg(NO_3)_2 + (NH_4)_2CO_3 + 3H_2O \longrightarrow MgCO_3 \cdot 3H_2O(s) + 2NH_4NO_3 \quad (2)$$

As soon as the addition of $(NH_4)_2CO_3$ brings the solution to the basic side, precipitation occurs.

The initial freeze-drying experiments were conducted by spraying solutions only several drops away from precipitation under the hypothesis that the carbonate complex would be strong enough to form during the rapid cooling. The basic approaches and results for forming the doped powders are summarized in Table I. A composition of 0.5 mole % CaO to MgO was selected for all experiments.

Work with the nitrates as outlined in Equations (1) and (2) resulted in a freeze-dried doped magnesium nitrate. This product was unsatisfactory for the intended purpose because of the molten phase which developed during heating. This resulted in a very large grained final MgO phase, and was judged unsuitable for hot pressing.

Experiments under approach number 2 were based on similar reasoning to that for number 1, but with the substitution of chloride salts. The results were completely analogous and the product was unsuitable for further experiments.

Sulphate was substituted for experiments under number 3, and with somewhat more encouraging results. A fluffy ammonium magnesium sulphate freeze-dried powder was obtained. Table II gives the results of calcinations followed by x-ray analysis.

TABLE I

EXPERIMENTS TO FORM UNIFORMLY Ca DOPED MgO

No.	Technique	Reactants	Dried Product	Calcined Product
1	Freeze-drying	$Mg(NO_3)_2$ + $(NH_4)_2CO_3$	$Mg(NO_3)_2 \cdot XH_2O$	Molten phase developed - unsatisfactory
2	Freeze-drying	$-Mg(Cl)_2$ + $(NH_4)_2CO_3$	$MgCl_2 \cdot XH_2O$	Molten phase developed - unsatisfactory
3	Freeze-drying	$-MgSO_4$ + $(NH_4)_2CO_3$	$(NH_4)_2Mg(SO_4)_2 \cdot 6H_2O$	MgO formed at about $1300°C$, but minor $CaSO_4$ and $5MgO \cdot MgSO_4 \cdot 8H_2O$ still present
4	Freeze-drying	$Mg(C_3H_3O_2)_2$ + $(NH_4)_2CO_3$	$Mg(C_3H_3O_2)_2 \cdot XH_2O$	MgO formed $<600°C$ - possibly satisfactory
5	Co-precipitation	$-Mg(NO_3)_2$ + $(NH_4)_2 \cdot CO_3$	$MgCO_3 \cdot XH_2O$	MgO formed $\leq 1100°C$ - satisfactory, possibly one unidentified phase

TABLE II

CALCINATION RESULTS FOR FREEZE-DRIED $(NH_4)_2Mg(SO_4)_2 \cdot 6H_2O$

| Calcination Temp., °C	Phase Analysis	
	Major	Minor
1000	$MgSO_4 \cdot 6H_2O$, $MgSO_4$	MgO
1100	$MgSO_4 \cdot 6H_2O$, $MgSO_4$	MgO
1300	MgO	$CaSO_4$, $5MgO \cdot MgSO_4 \cdot 8H_2O$

The sulphate and water radicals are so strongly bonded that even $1300^{\circ}C$ was not high enough to complete the calcination.

The development of a distinguishable $CaSO_4$ was somewhat disturbing and suggested inhomogeneous calcium distribution. In addition to this, the $1300^{\circ}C$ calcined product had a crystallite size in excess of 1 micron. For these reasons this approach was dropped from further consideration.

Examination of the literature has not suggested the use of acetates for freeze-drying. However, experiments were conducted as noted under approach number 4 on the basis that if the desired $MgCO_3$ was not obtained $Mg(C_3H_3O_2)_2$ itself decomposes to MgO at $320^{\circ}C$. Again, the carbonate complex was not strong enough to form during freeze drying. The Ca-doped $Mg(C_3H_3O_2)_2 \cdot XH_2O$ did calcine nicely giving an 80-90 A$^{\circ}$ MgO crystallite size as determined by x-ray line braodening after only 15 minutes at $600^{\circ}C$. The approach appears quite promising although consolidated specimens have not yet been made from this powder, and only after examining the dense microstructure can final judgement be passed. Additional batches could be made without the use of the $(NH_4)_2CO_3$.

Since techniques for forming $MgCO_3$ by freeze-drying were unsuccessful, co-precipitation experiments were conducted as noted in item 5. Ca-doped $MgCO_3$ was formed and this was calcined at $1100^{\circ}C$ for 1 hour which had previously been found to give an average 300 A$^{\circ}$ crystallite size. The powder was consolidated under conditions previously employed for high purity undoped.

The microstructure for the Ca-doped sample is compared with that for the high purity $MgCO_3$ in Figure 3. The sample containing CaO has a smaller grain size than the undoped sample. It is also noteworthy that this grain size is smaller than the moderate purity sample made from
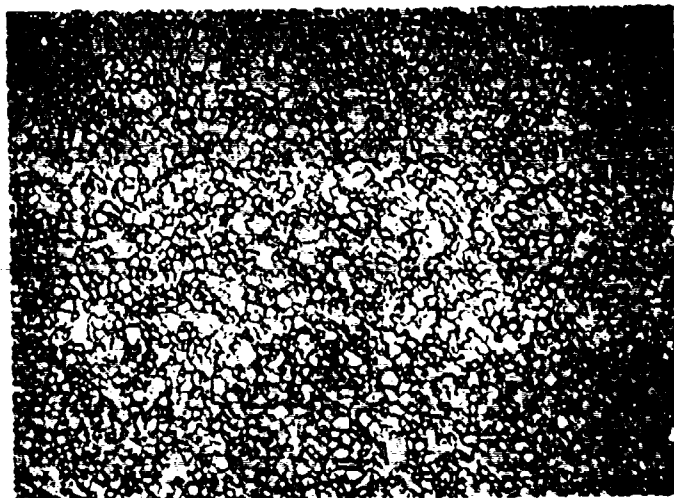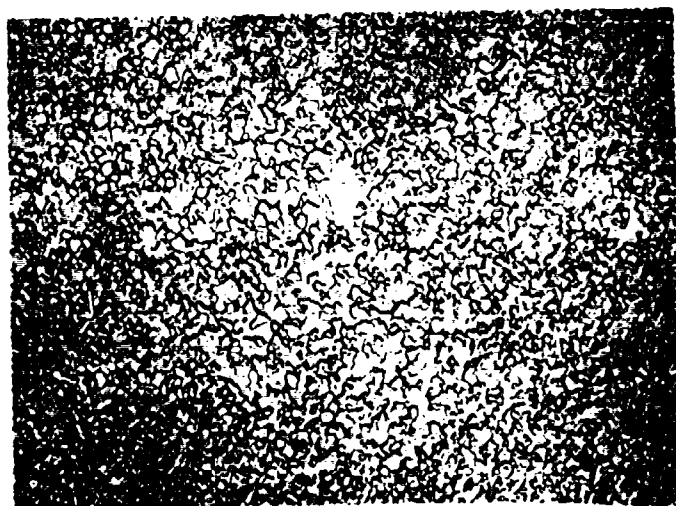
#5525-1   (a)   500X

Baker MgO $\longrightarrow$ MgCO$_3$ $\longrightarrow$ MgO + 0.5 mole % CaO
Static calcine 1100°C - 1 hr.

Hot Pressed

1250°C - 15 Kpsi - 90 min.
3.580 gm/cc - 2.9 μm
grain intercept

#5525-3   (b)   500X

SH182 Mg(OH)$_2$ $\longrightarrow$ MgCO$_3$ $\longrightarrow$ MgO
Static calcined 1100°C - 1 hr.

Hot Pressed

1250°C - 15 Kpsi - 90 min.
3.566 gm/cc - 3.4 μm
grain intercept

Figure 3. Microstructure of Hot Pressed Carbonate Derived MgO Prepared, (a) by Co-precipitation with 0.5 mole % CaO and (b) High Purity Undoped Powder.

Honeywell M-10 powder (Figure 2). All three samples were processed at the same temperature so any grain size variations due to process fluctuations should be randomized. Thus, the fact that the sample which one predicts would have the smallest grain size does indeed possess the smallest size suggests that the Ca acted as a grain boundary impurity drag during the late stages of the consolidation cycle. It was not possible to find a discrete second phase attributable to CaO by light microscopy techniques.

The specimen was fractured and an electron microscopy replica examination was conducted. Figure 4a illustrates a microstructure which is near to or possibly fully equiaxed. This is taken as evidence for a uniform distribution of dopant. Numerous singularities are apparent on Figure 4a and higher magnification views of the structure shown in Figure 4b. The central grain in Figure 4b has discrete islands of (arrow A) apparent second phase on what is probably a grain face. This would suggest that the second phase is non-wetting. However, grain boundaries which are at approximate right angles to the grain face show an apparent wide continuous phase (arrow B). A dihedral angle of 65° was estimated from one triple point intersection (arrow C). This, of course, is indicative of a partially penetrating second phase which is consistent with the second phase islands on grain faces. Additional examples of wide grain boundary phases are shown in Figure 4b (arrow D).

Undoped MgO specimens were examined by identical techniques and found to be free of grain boundary phase, thus, the correlation of the second phase with the deliberate doping appears justified. Using the diffusion rate for Ca^{+2} in MgO measured by Wuensch and Vasilos,[28] an estimate was made of the redistribution of the solute during consolidation. Using a
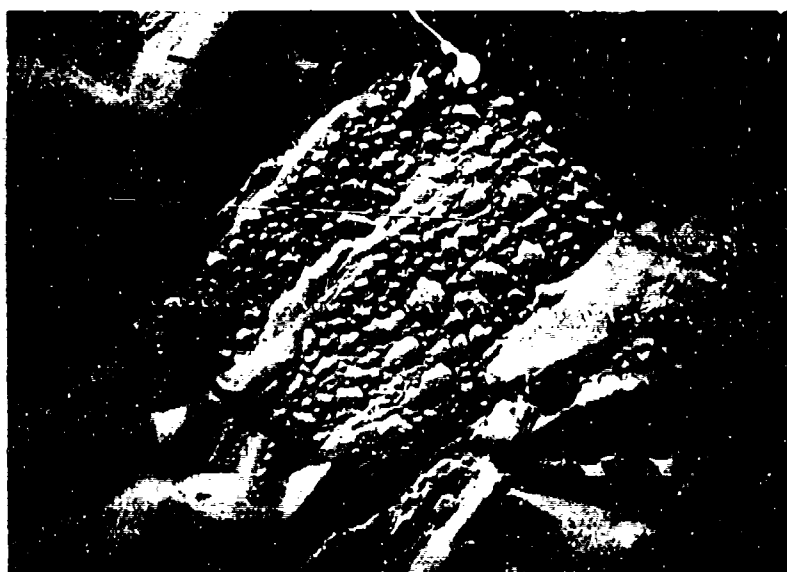
#71515   (a)   7500X

#71517   (b)   15,000X

Figure 4.   Fractographs of 0.5 mole % CaO Doped MgO Showing,
(a) Equiaxed Structure and (b) Second Phase.

graphical plot of Ficks' 2nd Law with spherical boundary conditions, it was estimated that redistribution would be 95% complete at 1250°C (the consolidation temperature) for a 3 μm crystallite size. The starting particle size was approximately 0.03 μm and the final size was 4.5 μm. Thus, it would appear safe to conclude that diffusion was not rate limiting and the cause of the observed grain boundary second phase. It is well known that CaO has limited solid solubility in MgO and limits of 3.5%, 1.1% and 0.9% CaO were established at 2015, 1820 and 1620°C, respectively.[29] An extrapolation of this data to 1250°C would establish a limit of about 0.6% CaO. Thus, it would appear that limited solid solubility of CaO was not the cause of the second phase. In fact, only several speculative explanations appear obvious; 1) selective precipitation of CaO leading to a concentration greater than 0.5% and even considerably above the solid solubility limit in the starting powder, 2) combination of CaO with another impurity, say SiO_2, to give an apparent high volume second phase, or 3) a high segregation coefficient leading to a concentration of the dopant at the grain boundary even though it is within the solubility limit. The work of Leipold[1] has given evidence for the combination of $Ca^{+2} + Si^{+4}$ in MgO grain boundary phases and high segregation coefficients. Property measurements could begin on this sample, but it is clear that this must be accompanied by further characterization of the grain boundary phase.

V. CONCLUSIONS

1. Fine uniform high purity, high density MgO specimens can be hot pressed from $MgCO_3$-derived MgO powder. The normal grain size distribution developed during consolidation was concluded to be due to the random crystallographic orientation of crystallites within an agglomerate and the entire powder compact. This is contrasted with $Mg(OH)_2$

derived powder where the decomposed MgO crystallites have at best a small angle grain boundary mis-orientation within an agglomerate which during consolidation undergo rapid grain growth leading to a dramatic abnormal microstructure. It was concluded that differences in the impurity level of the starting salts was not the cause of this behavior.

2. Adsorbed volatile species such as OH^- or CO_3^{-2} play little role in microstructure development in a 99.96% pure MgO-derived from $MgCO_3$; however, the possible role of such species on properties has not been ruled out.

3. Freeze-dried $MgCO_3$ cannot be easily obtained.

4. For the preparation of freeze-dried doped fine particulate MgO, $Mg(C_3H_3O_2)_2$ appears to be most suitable salt followed by $MgSO_4$. The latter does not completely decompose even at $1300^\circ C$ which also results in coarse crystallites.

5. Calcia-doped $MgCO_3$ can easily be prepared by co-precipitation and equiaxed dense samples were fabricated from such powder. Evidence was obtained for "impurity drag" to limit grain growth during consolidation.

6. Evidence was obtained for a partially penetrating grain boundary second phase. The amount of second phase seems excessive based on known solid solubility limits and the kinetics of the thermal cycle; however, several possible explanations were advanced. Further characterization of the second phase is required in conjunction with the property measurements.

VI. REFERENCES

1. M.H. Leipold, J. Am. Ceram. Soc., 49, 498 (1966).

2. B.J. Wuensch and T. Vasilos, J. Am. Ceram. Soc., 49, 433 (1966).

3. R.J. Stokes, J. Am. Ceram. Soc., 48, 60 (1965).

4. R.S. Gordon and W.D. Kingery, J. Am. Ceram. Soc., 49, 654 (1966).

5. W.H. Rhodes, B.J. Wuensch and T. Vasilos, First Annual
   Report, AVSD-0024-71-CR, Contract N00014-70-C-0138.

6. D. Turnbull, Trans. AIME, 191, 661 (1951).

7. W.D. Kingery and B. Francois, J. Am. Ceram. Soc., 48, 546 (1965).

8. F.A. Nichols, J. Appl. Phys., 37, 4599 (1966).

9. J.W. Cahn, Acta. Met., 10, 789 (1962).

10. M. Hillert, Acta. Met., 13, 227 (1965).

11. R.J. Brook, J. Am. Ceram. Soc., 52, 56 (1969).

12. A.U. Daniels, R.C. Lowrie, R.L. Gibby and I. Cutler, J. Am.
    Ceram. Soc., 45, 282 (1962).

13. R.M. Spriggs, L.A. Brissette and T. Vasilos, J. Am. Ceram. Soc.,
    47, 417 (1964).

14. G.C. Nicholson, J. Am. Ceram. Soc., 49, 47 (1966).

15. R.S. Gordon, D.D. Marchant and G.W. Holldenberg, J. Am. Ceram.
    Soc., 53, 399 (1970).

16. W.H. Rhodes, and R.M. Cannon, "Microstructure Studies of
    Refractory Polycrystalline Oxides," AVSD-0192-71-CR, Contract
    N00019-70-C-0171, February 1971.

17. R.J. Charles, "Fracture," edited by Averbach et al, John Wiley
    and Sons, New York, New York, p. 225 (1959).

18. F.J.P. Clarke and R.A.J. Sambell, Phil. Mag., 5, 897 (1960).

19. R.J. Stokes and C.H. Li, J. Am. Ceram. Soc., 46, 423 (1963).

20. R. Rice, Contract No. NAS-7-726, Progress Report No. 14,
    October 1967.

21. A.R. Westwood, D.L. Goldheim and R.G. Lve, Phil. Mag., 16,
    505 (1967).

VI. REFERENCES (Concl'd)

22. J.H. Westbrook and P.J. Jorgensen, Trans. AIME, 233, 425 (1965).

23. W.B. Hillig, R.J. Charles, from High Strength Materials, J. Wiley and Sons, New York (1965), p. 682.

24. F. Schuckler in Quantitative Microscopy edited by R.T. Deltoff and F.N. Rhines, McGraw-Hill (1968), p. 201.

25. R.W. Rice, Proc. Brit. Ceram. Soc., 99 (1969).

26. F.J. Schnettler, F.R. Monforte and W.W. Rhodes, Science of Ceramics, 4, 79 (1968).

27. D.W. Johnson and F.J. Schnettler, J. Am. Ceram. Soc., 53, 440 (1970).

28. B.J. Wuensch and T. Vasilos, NBS Spec. Publ. 296, 95 (1968).

29. R.C. Doman, J.B. Barr, R.N. McNally and A.M. Alper, J. Am. Ceram. Soc., 46, 313 (1963).